

The Contribution of Active Galactic Nuclei to the Microjansky Radio Population

D. R. Ballantyne

Center for Relativistic Astrophysics, School of Physics, Georgia Institute of Technology, Atlanta, GA 30332; david.ballantyne@physics.gatech.edu

ABSTRACT

A X-ray background synthesis model is used to calculate the contribution of Active Galactic Nuclei (AGNs) to the 1.4 GHz number counts between 100 nJy and 10 mJy. The number counts are broken down into contributions from radio-quiet and radio-loud AGNs, obscured and unobscured AGNs, and for different ranges in redshift and 2–10 keV X-ray luminosity, L_X . Compton-thick AGNs are included, but only to the level required to fit the peak of the X-ray background. The predicted radio counts show that the μJy AGN population will be dominated by obscured, radio-quiet Seyfert galaxies with $\log L_X < 43$, and spanning $0 < z \lesssim 3$. However, depending on the exact relationship between the radio and X-ray luminosities in radio-quiet AGNs, additional radio flux due to star-formation within AGN host galaxies may be necessary in order to match the observed AGN counts at a flux density of $\sim 50 \mu\text{Jy}$. The star-formation rates (SFR) required are modest, only $\sim 3 M_\odot \text{ yr}^{-1}$, assuming a constant rate with z and L_X . A more observationally and theoretically motivated relationship, where the $\text{SFR} \propto (1+z)^{1.76}(\log L_X - 40)^{3.5}$, will also account for the observed counts. The μJy AGN population will provide a very clean sample to trace the accretion and galactic star-formation histories of Seyfert galaxies over a significant fraction of cosmic time.

Subject headings: galaxies: active — galaxies: evolution — galaxies: Seyfert — galaxies: starburst — radio continuum: galaxies

1. Introduction

The identification of powerful radio sources with quasi-stellar objects in the 1960s (Matthews & Sandage 1963; Hazard et al. 1963; Schmidt 1963) ultimately led to the realization that Active Galactic Nuclei (AGNs) were the locations of accreting supermassive

black holes (e.g., Salpeter 1964; Lynden-Bell 1969). Since that time, radio observations have continued to be an important probe of the AGN phenomenon, especially in the investigation of relativistic jets emanating from the central engine (e.g., Bridle & Perley 1984; Kellermann & Owen 1988; O’Dea 2002). The next decade will see a major leap forward of the capabilities of centimeter wave radio instrumentation with the development of the Expanded-VLA (EVLA; Napier 2006) and, ultimately, the Square Kilometer Array¹. The increase in sensitivity afforded by these new instruments will probe the radio population down to flux densities less than a μJy , opening a new window into the study of AGN evolution and the growth of supermassive black holes.

At flux densities $S \gtrsim 1 \text{ mJy}$, the radio source population is dominated by radio-loud AGNs, and it has long been known that the number count distribution indicates strong cosmic evolution (e.g., Longair 1966; Condon 1984, 1989). However, the radio number counts significantly flatten at fluxes below 1 mJy (e.g., Condon 1984; Windhorst et al. 1985; Hopkins et al. 1998; Richards 2000; Seymour et al. 2004; Simpson et al. 2006; Kellermann et al. 2008) indicating either a sudden change in evolutionary properties, or, more likely, the appearance of a new population of sources such as emission from star-forming galaxies (e.g., Windhorst et al. 1995; Benn et al. 1993; Richards 2000; Seymour et al. 2004). Strong radio emission from star-forming regions is expected as supernova remnants will accelerate cosmic rays which will radiate synchrotron emission in local magnetic fields. At low redshifts, the radio and far-infrared powers of star-forming galaxies are tightly correlated, allowing for the radio luminosity to act as a star-formation rate (SFR) indicator (Condon 1992; Yun et al. 2001; Bell 2003). This correlation seems to hold at higher redshifts (Beswick et al. 2008; Ibar et al. 2008; Garn & Alexander 2009).

In recent years, several surveys have continued to probe the radio source population to ever-smaller values (e.g., Hopkins et al. 2003; Simpson et al. 2006; Schinnerer et al. 2007; Kellermann et al. 2008), with the deepest VLA surveys reaching rms noise levels of only a few μJy per beam. Matching the radio sources to complementary optical, X-ray and infrared surveys has allowed the properties of many of the faintest radio sources to be estimated (Seymour et al. 2008; Smolčić et al. 2008; Padovani et al. 2009). The results of these studies, while still with large error-bars, indicate that radio-quiet AGNs may make up to one-third of the radio source population below 100 μJy (Padovani et al. 2009). As $\sim 90\%$ of AGNs are radio-quiet, these results imply that the deep radio surveys are now uncovering the dominant population of active galaxies.

The last decade has provided a wealth of new data tracing the evolution of supermassive

¹<http://www.skatelescope.org>

black holes and their impact on galaxy formation (e.g., Kauffmann et al. 2003; Grogin et al. 2005; Pierce et al. 2007; Silverman et al. 2008a; Gabor et al. 2009; Schawinski et al. 2009; Hickox et al. 2009), but it has proved difficult to simultaneously study the AGN and host galaxy. Galaxies are much less luminous than AGNs at X-ray energies, so deep X-ray observations are very efficient at finding all but the most heavily obscured AGNs over a wide range of redshift and luminosity (Mushotzky 2004; Brandt & Hasinger 2005). These surveys have showed that the vast majority of AGNs in the Universe are absorbed, and that AGNs evolve in the same form of ‘cosmic downsizing’ as the galaxy population (e.g., Ueda et al. 2003; Barger et al. 2005). However, aside from indirect inferences using the evolution of the X-ray absorber (Ballantyne et al. 2006), it is very challenging to glean much information about the affect of the AGN on the host galaxy through X-ray observations. Optical, ultraviolet, and infrared wavelengths allow study of both the host galaxy and AGN, but the extinction and re-emission properties of dust in the host galaxy severely complicate the interpretation when, as is nearly always the case, the galaxy is not spatially resolved (e.g., Moran et al. 2002; Donley et al. 2008). The radio regime is unique in that it provides a nearly uncorrupted view of both processes. All AGNs produce some form of non-thermal nuclear radio emission which, although weak, can be identified by its high brightness temperature (e.g., Hutchings & Neff 1992; Blundell et al. 1996; Kukula et al. 1998) and is immune to attenuation by any circumnuclear torus. Radio-emission from the host galaxy will provide a similarly unabsorbed view into ongoing star-formation. Thus, combining studies of the μJy radio-quiet AGN population with other multiwavelength surveys will allow a relatively clean look into the combined problem of AGN and galaxy evolution.

In this paper, we make use of a X-ray background synthesis model to predict the number counts of radio-quiet AGNs down to a flux density of 100 nJy. The calculations break down the contribution of AGNs from different redshifts and nuclear luminosities. In addition, we add in radio-emission from various levels of star-formation in the AGN host galaxies to explore the impact on the predicted number counts. The next section describes the calculations necessary to move from a X-ray background synthesis model to predicting the radio number counts. Section 3 then presents and describes the results, including the effects of adding in star-formation. The results are discussed and summarized in Section 4. The following Λ -dominated cosmology is assumed in this paper: $H_0 = 70 \text{ km s}^{-1} \text{ Mpc}^{-1}$, $\Omega_\Lambda = 0.7$, and $\Omega_m = 0.3$ (Spergel et al. 2003). The flux density of a radio source has a spectral index α , so that $S \propto \nu^\alpha$.

2. Calculations

Previously, Jarvis & Rawlings (2004) and Wilman et al. (2008) estimated the radio-quiet AGN contribution to the radio counts by employing the Ueda et al. (2003) hard X-ray luminosity function, multiplying by a constant to correct for Compton-thick AGNs, and then employing a *ROSAT*-based correlation (Brinkmann et al. 2000) to convert from X-ray to radio luminosity. In both these papers, they use separate radio-derived luminosity functions to account for radio-loud AGNs. Below, we present a new method to estimate the radio-quiet AGN number counts that will improve on this previous work in several ways. First, we base our calculations on a fit to the X-ray background. This allows the peak spectral intensity of the background at ~ 30 keV to be used as a constraint on the missing Compton-thick fraction, and has the added feature of allowing us to break down the number counts into contributions from different groups such as obscured AGNs, or ones in a specific redshift or luminosity range. Furthermore, we account for a radio-loud fraction of AGN. The X-ray luminosity function counts both radio-loud and radio-quiet AGNs, so the radio-loud fraction must be subtracted from the total before predicting the radio-quiet counts. Finally, we convert from X-ray to radio luminosity using a luminosity-dependent conversion factor derived from high-resolution radio and hard X-ray observations of the nuclear regions of nearby AGNs. While clearly there remain several uncertainties in the steps described below, the changes outlined above should result in a more accurate prediction of the AGN contribution to the deep radio counts. In these calculations, an AGN is assumed to be obscured if it is attenuated by a hydrogen column $N_{\text{H}} \geq 10^{22} \text{ cm}^{-2}$.

2.1. The X-ray Background Synthesis Model

The hard X-ray background encodes within it the entire history of accretion onto supermassive black holes, independent of whether or not an individual AGN is radio-loud or radio-quiet. A detailed description of the X-ray background synthesis model employed here is beyond the scope of the current paper, and, indeed, many aspects of the model such as the X-ray spectral shapes, and the distribution of column densities have no impact on the predicted radio number counts. For this application the important ingredients of the model are the absorption-corrected hard X-ray luminosity function, and the obscured-to-unobscured AGN ratio (i.e., the ratio of type 2 AGNs to type 1 AGNs). The Ueda et al. (2003) hard X-ray luminosity function is the basis for the calculations presented here.

The AGN type 2/type 1 ratio is observed to significantly decrease with AGN luminosity (Ueda et al. 2003; La Franca et al. 2005; Simpson 2005; Akylas et al. 2006; Treister et al. 2008). The explanation for this effect is not entirely understood, but is most likely related to

the increased outward radiation pressure produced at high AGN luminosities (Lawrence 1991; Simpson 2005). The best determination of the local ($z \sim 0$) dependence of the AGN type 2/type 1 ratio with luminosity was produced by the *Swift*/BAT detector in the 14–195 keV band (Tueller et al. 2008). AGN selection at these energies is expected to be completely unbiased to objects with Compton-thin absorbers. Figure 1 plots the BAT AGN type 2 fractions, f_2 as a function of $L_X = L_{2-10 \text{ keV}}$ where the conversion $\log L_X \approx 1.06 \log L_{14-195 \text{ keV}} - 3.08$ found by Winter et al. (2009) was used to convert the BAT luminosities to L_X . The plot shows a strong trend of an increasing fraction of obscured AGNs as the nuclear luminosity decreases. The lowest luminosity point indicates a much lower obscured fraction than expected by this trend, but lies at such low luminosity that it is likely contaminated by LINERs and other low-luminosity AGNs that have significantly different nuclear environments and evolutionary histories than rapidly accreting AGNs at higher luminosities (Ho 2008). In practice, the hard X-ray luminosity functions are integrated down to $\log L_X = 41.5$. A power-law of the form $f_2 \propto L_X^{-\beta}$ was fit to the data with the normalization set by the type 2/type 1 ratio at $\log L_X = 41.5$. The lowest luminosity datum was included in the fit, but its removal makes a negligible impact on the results. Assuming an obscured-to-unobscured ratio of 4:1 at $\log L_X = 41.5$, the best-fit (reduced $\chi^2 = 0.97$) was found for $\beta = 10.5$. The predicted radio number counts decrease by only 6% if the smooth step function shown by Tueller et al. (2008) is used to describe the variation in f_2 .

This description of the AGN type 2 fraction is based on observations of local AGNs, but there is now accumulating evidence that f_2 also increases with redshift as $(1+z)^\gamma$ (La Franca et al. 2005; Ballantyne et al. 2006; Treister & Urry 2006; Hasinger 2008). This finding is still controversial (Dwelly & Page 2006), and the data is not yet at the point to determine if there is a luminosity dependence to γ . Here, we assume $\gamma = 0.4$, a value consistent with the various estimates, and that the AGN type 2 fraction evolves out to $z = 1$, where, in analogy with the cosmic star-formation rate density (e.g., Hopkins 2004; Hopkins & Beacom 2006), it flattens to $\gamma = 0$. If we instead choose $\gamma = 0.62$ with the evolution continuing to $z = 2$ (Hasinger 2008), then the predicted radio counts increase by only 8%.

The hard X-ray luminosity functions derived in the literature are based on observations at energies less than ~ 10 keV, and so are insensitive to Compton-thick AGNs, those with absorbing column densities $N_H \gtrsim 10^{24} \text{ cm}^{-2}$. Therefore, the unknown fraction of Compton-thick AGNs has to be included ‘by hand’ into any X-ray background model in order to fit the peak of the spectrum at ~ 30 keV. For the Ueda et al. (2003) X-ray luminosity function, it was found that a Compton-thick fraction equal to the fraction of Compton-thin type 2 AGNs provided a very good fit to the peak of the X-ray background. That is, at every z and L_X , the Compton-thick AGN fraction was equal to f_2 . The implicit assumption is that

the Compton-thick population evolves in the same manner as the Compton-thin AGNs.

2.2. Translating the X-rays to Radio

The X-ray background model provides the number density of obscured and unobscured AGNs as a function of z and L_X . To calculate how these AGNs appear in the radio sky, the X-ray luminosity must first be translated into radio luminosities, which, for radio-quiet AGNs, is not necessarily straightforward. Previous work by Jarvis & Rawlings (2004) and Wilman et al. (2008) made use of the correlation published by Brinkmann et al. (2000) based on AGNs selected through cross-correlating the *ROSAT* All-Sky Survey and the FIRST 1.4 GHz radio catalogue. However, it is not clear if this correlation is valid over a wide range of AGN luminosities. The *ROSAT* All-Sky Survey was a shallow, soft X-ray survey and the sources selected by Brinkmann et al. (2000) are typically unobscured, luminous quasars. These objects lie at substantial redshifts ($z > 0.1$) and therefore it is possible that the radio emission in the FIRST beam may be contaminated by star-formation in the host galaxies. As we are interested in the relationship between the core X-ray and radio luminosities, it would be best to use results based on observations of lower-luminosity radio-quiet AGNs that have isolated the nuclear radio emission.

Therefore, we consider the results of Terashima & Wilson (2003) and Panessa et al. (2007) who studied the X-ray and radio nuclear luminosities of nearby AGNs with high resolution observations. The Panessa et al. (2007) sample was limited to low luminosity Seyfert galaxies and LINERs with $\log L_X < 43$, with many of the AGNs accreting at very low rates with respect to the Eddington limit. This is problematic because it is now known that radio-loudness is more common at low accretion rates (Terashima & Wilson 2003; Panessa et al. 2007; Sikora et al. 2007), so a sample of low luminosity AGN may be biased toward high radio luminosities. In contrast, Terashima & Wilson (2003) plot the AGN radio to X-ray luminosity ratio as a function of L_X over a wide range of X-ray luminosities. Although there is a scatter of ~ 0.5 dex, they find that it decreases with L_X until it reaches a minimum at $\log L_X \approx 43$ –44 before increasing again. Defining $R_X = \log \nu L_\nu(5 \text{ GHz}) / \log L_X$ we quantify this behavior as

$$R_X = \begin{cases} -0.67 \log L_X + 23.67 & 41.5 \leq \log L_X \leq 43 \\ -5 & 43 < \log L_X \leq 44 \\ \log L_X - 49 & 44 < \log L_X \leq 45 \\ -4 & \log L_X > 45 \end{cases} \quad (1)$$

This is the relationship used to convert from the X-ray to the rest-frame 5 GHz radio luminosity. To calculate the observed flux at 1.4 GHz, a spectral index of $\alpha = -0.7$ is assumed

(Kukula et al. 1998). In Sect. 3.2, we will show how the results change if the Panessa et al. (2007) relationship is used for all luminosities.

The X-ray to radio conversion for the radio-loud population is also derived from Terashima & Wilson (2003): $\nu L_\nu(5 \text{ GHz}) \approx 10^{-2} L_X$. This proportionality factor has a scatter of ~ 1 dex, but, as is seen below, the radio-loud population does not impact our conclusions, as they comprise a negligible component of the radio population at μJy levels. A spectral index of $\alpha = -0.8$ is assumed to calculate the observed 1.4 GHz fluxes of radio-loud AGNs.

The small fraction of radio-loud AGNs has to be removed from the entire X-ray selected population to concentrate on the properties of the dominant radio-quiet AGNs below 100 μJy . As mentioned above, radio-loud AGNs are most common at high luminosity (the radio-loud quasars) and at very low nuclear luminosities, but these latter objects are not important to the X-ray background and are omitted here. At every z , the radio-loud fraction is assumed to rise exponentially from $\log L_X = 41.5$ to 46: $f_{\text{RL}} = c \exp(\log L_X - 40) + b$. A decent fit to the radio number counts between 1 and 10 mJy was found assuming $f_{\text{RL}} = 0.0175$ at $\log L_X = 41.5$ and $f_{\text{RL}} = 0.10$ at $\log L_X \geq 46$. These values are consistent with the canonical AGN radio-loud fraction of 10–20% (e.g., Donoso et al. 2009).

The 1.4 GHz radio number counts are commonly displayed as the differential counts, dN/dS . This can be related back to the X-ray band by

$$\frac{dN}{dS} = \frac{dN}{d \log L_X} \frac{d \log L_X}{dS}, \quad (2)$$

where

$$\frac{dN}{d \log L_X} = \frac{c}{H_0} \int_{z_{\min}}^{z_{\max}} \frac{d\Phi(L_X(\min), z)}{d \log L_X} \frac{d_l^2}{(1+z)^2 (\Omega_m (1+z)^3 + \Omega_\Lambda)^{1/2}} dz. \quad (3)$$

In this last expression $d\Phi(L_X(\min), z)/d \log L_X$ is the hard X-ray luminosity function, d_l is the luminosity distance, and $L_X(\min)$ is the minimum X-ray luminosity that can produce a given 1.4 GHz radio flux S . The radio flux S is related to the rest-frame 1.4 GHz luminosity L_ν by

$$S = \frac{L_\nu (1+z)^{1+\alpha}}{4\pi d_l^2}. \quad (4)$$

The last factor in equation 2, $d \log L_X/dS$, cannot be expressed analytically (especially when additional flux due to star-formation is included), and is calculated numerically.

Thus, for a given S , the integral in equation 3 is calculated from $z_{\min} = 0$ to $z_{\max} = 5$ with a new value of $L_X(\min)$ for each evaluation of the integrand. Separate calculations are performed for radio-quiet type 1 AGNs, radio-loud type 1 AGNs, radio-quiet type 2 AGNs, and radio-loud type 2 AGNs. The total 1.4 GHz dN/dS is then the sum of the results of the four individual calculations.

3. Results

The solid line in Figure 2 plots the predicted Euclidean-normalized radio counts from AGNs at 1.4 GHz. In this figure the contributions from obscured, type 2 AGNs and unobscured, type 1 AGNs are indicated by the dotted and short-dashed lines, respectively. Obscured AGNs dominate the predicted radio number counts from $0.1 \mu\text{Jy}$ to 10 mJy by factors $\gtrsim 3$. This result is independent of the details of any of the modeling and is a very general conclusion. The X-ray background requires type 2 AGNs to outnumber type 1s at all but the highest luminosities (see Figure 1), and this fact immediately translates to the radio number counts. Therefore, AGNs detected at μJy flux levels by the EVLA or the SKA will very likely be obscured type 2 objects.

The black symbols in Figure 2 plot the observed total 1.4 GHz number counts taken from various published surveys over the last decade. The flattening of the counts at fluxes below 1 mJy is reproduced by every dataset. By construction the predicted counts pass through the majority of the data points for $S > 1 \text{ mJy}$, as radio-loud AGNs dominate this regime, and the radio-loud fraction was determined by matching the model to the mJy data. At lower flux densities the model passes well below the observed data, but this is to be expected as star-forming galaxies should dominate the μJy radio counts (Gruppioni et al. 2003; Huynh et al. 2005). However, the model also significantly underpredicts (by a factor of ~ 5 at $30 \mu\text{Jy}$) the estimated number counts due to AGNs (the red and blue data, taken from Padovani et al. (2009) and Seymour et al. (2008), respectively). Therefore, our baseline model that is derived from an accurate fit to the X-ray background cannot account for the observed AGN number counts in the latest deep radio surveys.

Figure 2 illustrates that the problem in the modeling arises from the contribution of radio-quiet AGNs. Radio-loud AGNs, denoted by the dot-dashed-line in the figure, are fixed by the mJy population and cannot help make up the deficit at $S < 100 \mu\text{Jy}$ unless the radio-loud population evolves very differently than what is currently observed. Padovani et al. (2009) estimated the radio-quiet AGN contribution to the 1.4 GHz number counts in the CDF-S field, and these are plotted as the cyan data. The model radio-quiet population underpredicts the observed estimates by factors of ~ 3 – 5 .

The breakdown of the 1.4 GHz number counts into AGNs of differing X-ray luminosities is shown in Figure 3. When $S \gtrsim 1 \text{ mJy}$, the radio counts are dominated by moderately-luminous radio-loud AGNs with $\log L_X \geq 43$. The radio-quiet population at lower flux densities is dominated by low luminosity Seyfert galaxies. Indeed, AGNs with X-ray luminosities $\log L_X < 43$ comprise the largest fraction of the radio-quiet number counts. This fact explains why obscured AGNs are the greatest contributor to the number counts at μJy fluxes.

The dependence of the AGN 1.4 GHz counts on source redshift is shown in Figure 4. Not surprisingly, the radio-loud AGNs are predominately found at $1 \leq z \leq 3$ where higher luminosity AGNs are more common. However, once the radio-quiet population starts dominating the counts at $S \lesssim 100 \mu\text{Jy}$, we find that Seyfert galaxies at $z < 1$ are the most common contributor to the radio-quiet AGN counts for $0.5 \lesssim S \lesssim 100 \mu\text{Jy}$, but at lower fluxes the counts are dominated by increasingly more distant AGNs. This behavior is in contrast to models of the radio-counts where pushing to fainter and fainter flux limits only reveals less luminous sources at roughly the same distance (Condon 1989). Figures 3 and 4 show that this is not the case for radio surveys of AGNs. In fact, these calculations show that μJy radio observations will be a good probe of tracing the evolution of Seyfert galaxies over a large fraction of cosmic time.

The above results have shown that the predicted 1.4 GHz radio counts from radio-quiet AGNs are $\sim 5\times$ too low when compared against the latest estimates from deep surveys. One way of increasing the model AGN radio counts is to add further Compton-thick AGNs. If the additional Compton-thick AGNs had very large columns with $\log N_{\text{H}} \gtrsim 25$ then, in principle, the X-ray background would be insensitive to their presence. However, the Compton-thick fraction has to be increased to 10 times the number of Compton-thin type 2s in order to bring the radio-quiet number counts to the level estimated by Padovani et al. (2009). Even if all these Compton-thick AGNs has column densities $\log N_{\text{H}} > 25$, the peak intensity of the X-ray background spectrum would be grossly overestimated. We conclude that a large population of hidden Compton-thick AGNs can not account for the deficit in the predicted 1.4 GHz counts.

3.1. The Role of Star Formation

A natural way to increase the radio luminosity from AGNs is to have ongoing star-formation in the host galaxy. The fact that the AGNs contributing to the μJy radio emission have significant nuclear obscuration is also a clue that star-formation may be important, as it may play a significant role in obscuring Seyfert galaxies at $z \sim 1$ (Fabian et al. 1998; Wada & Norman 2002; Thompson et al. 2005; Ballantyne 2008). The calibration of Bell (2003) is used to calculate the 1.4 GHz radio luminosity from a given SFR, and $\alpha = -0.8$ is assumed for the radio spectrum of the star-forming regions (Yun et al. 2001). To calculate the number counts with both AGN and star-formation emission, the star-forming 1.4 GHz flux at a given SFR and z is added to the AGN flux, and then the integral in equation 3 is computed as before. As type 2 AGNs dominate the AGN radio counts at all fluxes (see Fig. 2), emission from star-formation was only added when calculating the total flux of

obscured AGNs. Calculations including star-formation in type 1 AGNs had no impact on the results. Likewise, although the star-forming radio flux was added to the radio-loud population, the AGN component easily overwhelmed the emission from star-formation and the counts at $S \gtrsim 1$ mJy did not change.

The black curves in Figure 5 show the predicted 1.4 GHz radio counts when a constant SFR of $3 M_{\odot} \text{ yr}^{-1}$ was assumed for all obscured AGNs, independent of L_X or z . With this simple addition the model is now very close to the observed estimates of both the total and radio-quiet AGN contribution. This modest SFR would not be out of place in the Milky Way (Solomon & Sage 1988), and is consistent with constraints from the cosmic infrared background (Ballantyne & Papovich 2007). The fact that adding such a moderate amount of star-formation in AGN host galaxies can bring the models in line with the data is strong evidence that such levels of star-formation is common in the host galaxies of obscured AGNs at $z \gtrsim 0.5$ (Silverman et al. 2009). Moreover, the deep μJy radio surveys will be able to constrain the average SFRs in obscured AGNs and determine any dependence on luminosity and z .

As an illustration of what may be expected, we consider a SFR that is a function of both redshift and the AGN luminosity. The luminosity dependence may be expected if star-forming disks at distance ~ 100 pc from the central engine both obscure and feed the black hole (e.g., Shi et al. 2007; Watabe et al. 2008). In the analytic models of Ballantyne (2008), the maximum SFR found in these disks was proportional to the X-ray luminosity, so that less-luminous Seyfert galaxies required a lower SFR than more luminous AGNs. The reason is that to fuel a luminous AGN requires a significant gas supply that can also turn rapidly into stars. Using these results as a guide, the luminosity dependence seems to roughly follow $\text{SFR} \propto (\log L_X - 40)^{3.5}$.

To estimate the redshift dependence, we note that Kim et al. (2006) mention that the SDSS type 2 AGNs identified by Zakamska et al. (2003) have a $\text{SFR} \sim 20 M_{\odot} \text{ yr}^{-1}$ as judged by the [O II] line strength. The mean [O III] luminosity for their sample is $L_{[\text{O III}]} \approx 3 \times 10^{42} \text{ erg s}^{-1}$. Heckman et al. (2005) found that for local type 1 AGNs, the average ratio between L_X and $L_{[\text{O III}]}$ is 1.59 dex. These authors do not correct for absorption in their sample of type 2 AGNs to find the ratio for obscured AGNs, so we follow the AGN unified model and apply the type 1 conversion to the Zakamska et al. (2003) sample resulting in $L_X \approx 10^{44} \text{ erg s}^{-1}$. The majority of the SDSS objects are at $z \sim 0.3$ (Zakamska et al. 2003). Ballantyne (2008) found a $\text{SFR} \sim 40 M_{\odot} \text{ yr}^{-1}$ in a nuclear starburst disk fueling an AGN with $L_X \approx 10^{44} \text{ erg s}^{-1}$. If we assume that this situation is common at $z \sim 1$ (i.e., at the peak of the cosmic star-formation history), then the SFR in the AGN host galaxy varies as $(1+z)^{1.76}$. Surprisingly, this is comparable to the redshift dependence of the SFR in quasar

host galaxies inferred by Serjeant & Hatziminaoglou (2009) using a sample selected in the far-infrared; therefore, this redshift dependence does not seem unreasonable. As with the AGN type 2/type 1 ratio, the redshift evolution was halted at $z = 1$.

The normalization of the SFR evolution was adjusted to obtain an adequate looking fit to the radio data. The final evolutionary law is

$$\text{SFR} \approx 0.25(1+z)^{1.76}(\log L_X - 40)^{3.5} M_\odot \text{ yr}^{-1}, \quad (5)$$

for $z < 1$ (the SFR remains at the $z = 1$ values at larger redshifts) and is plotted in Figure 6. The redshift and luminosity dependences in equation 5 are steeper than those that were recently found by Silverman et al. (2009) by studying AGN hosts in the zCOSMOS survey. However, the scatter in the data is about an order of magnitude, and the predicted SFRs fall within the range observed in the zCOSMOS data. Given the uncertainties in both the modeling and observations, equation 5 should be considered as a reasonable, observationally-motivated suggestion for how the SFR in AGN host galaxies may evolve.

The 1.4 GHz radio counts from AGNs and their host galaxies, assuming a SFR following eq. 5, are shown as the green curves in Figure 5. The new predicted radio-counts pass through the majority of the observed data points. AGNs with $\log L_X < 43$ still provide the majority of the counts at $S < 100 \mu\text{Jy}$, but higher luminosity AGNs are now a significant contributor at $S \sim 40 \mu\text{Jy}$ (Figure 7). Comparing Figs. 7 and 3, we see that the star-formation has the largest impact on the counts only for AGNs with $\log L_X < 44$. This is because the radio-flux from the AGN grows faster with luminosity than the flux from the star-forming regions. The μJy counts will then be most sensitive to measuring the SFR in Seyfert galaxies.

With the addition of the redshift-dependent star-formation law, the redshift distribution of the AGN radio-counts spreads to higher fluxes (see Figure 8). In this model, radio-quiet AGNs at $z \leq 1$ are predicted to be common at $S \sim 40 \mu\text{Jy}$, as compared to the case with no star-formation where these AGNs peak at $S \sim 10 \mu\text{Jy}$ (Fig. 4). The planned EVLA surveys should measure the total radio-counts down to $\sim 1 \mu\text{Jy}$. Therefore, the evolution of star-formation in AGN host galaxies should, in principle, be measured by the deep EVLA surveys.

3.2. Is Star Formation Required?

The results presented above indicate that additional radio emission from star-forming regions in AGN host galaxies must be included in order for the predicted number counts to match the observations. However, this conclusion will depend on the choice of the X-ray to

radio conversion employed in the modeling. We have argued in Sect. 3 that a luminosity-dependent conversion factor (eq. 1) drawn from the work of Terashima & Wilson (2003) was the most appropriate choice. Padovani et al. (2009) found that their estimates of the radio-quiet contribution to the number counts were adequately described by a model with a luminosity-independent conversion factor consistent with the Brinkmann et al. (2000) relation. To test the sensitivity of our conclusions we therefore computed a new model of the 1.4 GHz radio counts using the Panessa et al. (2007) relationship derived from high-resolution observations of local low-luminosity Seyfert galaxies: $\log L_X \approx (0.97) \log \nu L_\nu(5 \text{ GHz}) + 5.23$. Figure 9 presents the results of this calculation and clearly shows that this model does a good job fitting the estimated AGN counts with no additional emission from star-formation. The contribution from radio-quiet AGNs is slightly overpredicted, but Padovani et al. (2009) state that size of the error-bars are most likely underestimated. While emission from star-formation in the AGN host galaxies is not required to match the data while using the Panessa et al. (2007) relation, a small ($\sim 2 M_\odot \text{ yr}^{-1}$) amount of star-formation in the host galaxies is still consistent with the observational constraints.

Figures 10 and 11 plot the contributions to the counts from AGNs in different luminosity and z bins in this scenario. A comparison between these figures and Figs. 7 and 8 show significant differences in the properties of AGNs that dominate the μJy counts. The Panessa et al. (2007) conversion results in larger radio luminosities for AGNs with $\log L_X \sim 43\text{--}44$ and, as these AGNs dominate the X-ray background (e.g., Ballantyne et al. 2006), they also dominate the μJy radio counts. This is in contrast with the model that requires star-formation where AGNs with $\log L_X \lesssim 43$ will be most common at these fluxes (Fig. 7). Similarly, Fig. 11 predicts that AGNs at $1 \leq z \leq 3$ will be equally common at μJy fluxes as AGNs at $z < 1$, while Fig. 8 shows that AGNs at $z < 1$ will dominate if there is significant star-formation within the host galaxies. Therefore, the luminosity and redshift distributions of the AGNs detected in the deep radio surveys may help indicate whether or not additional radio emission from star-formation is necessary to explain the count distribution. Recently, Tozzi et al. (2009) has examined the properties of X-ray sources in the *Chandra* Deep Field South that were also detected by the deep VLA survey of that region (Kellermann et al. 2008). Tozzi et al. (2009) found that the redshift distribution of the radio sources with X-ray counterparts was peaked at lower redshifts (median 0.73) than the X-ray sources without a radio match (median 1.03). This result is qualitatively consistent with the predictions of the AGN number counts that includes star-formation from the host galaxy (Fig. 8).

4. Discussion and Summary

The principle conclusion of this work is that, depending on the nature of the X-ray to radio conversion in radio-quiet AGNs, the observed radio number counts of AGNs indicate that moderate levels of star-formation exist in the radio-quiet μJy AGN population. Thus, deep radio surveys will be an important probe of the connection between galaxy and black-hole growth. In particular, combining μJy radio data with results from surveys at other wavelengths will probe how the star-formation properties of AGN host galaxies evolve with z .

The model of the radio-counts was based on a fit to the X-ray background spectrum and made use of the hard X-ray luminosity function. It was found that in almost all cases the μJy counts due to AGNs are dominated by Seyfert galaxies with $\log L_X < 43$. The radio flux produced by more luminous AGNs was swamped by the minority radio-loud population. The implication is that AGNs selected by their μJy radio emission will be overwhelmingly obscured Seyfert galaxies spread over a range of redshifts. Radio selection, therefore, will result in a way of probing the evolution of the low-luminosity end of the hard X-ray luminosity function. This will be especially interesting in light of recent suggestions that the evolutionary pathways may be very different for galaxies that host high-luminosity quasars and those that host Seyferts (e.g., Ballantyne et al. 2006; Hasinger 2008; Hickox et al. 2009). The idea here is that quasars are the signatures of the formation of massive galaxies generated by the violent mergers of two large gas-rich galaxies (e.g., Kaufmann & Haehnelt 2000; Hopkins et al. 2005). The lower-luminosity AGNs, such as Seyferts, do not require such large fueling rates, and may be signatures of a less violent path of galaxy assembly. Thus, the Seyfert galaxies found at μJy radio fluxes will be a simple way to select and measure the properties of AGNs and their host galaxies with little contamination from the higher luminosity population.

The results described in Sect. 3 show that moderate amounts of star-formation may be ongoing in the μJy AGN population. In addition, these AGNs will be overwhelmingly obscured, or type 2 AGNs. This is consistent with the idea that the absorbing medium around an AGN is related to the host galaxy SFR (e.g., Ballantyne 2008). A corollary of this scenario would be that the SFR and its associated radio-flux would be correlated with X-ray column density. There are some observational hints that this may be occurring: both Georgakakis et al. (2004) and Richards et al. (2007) found an increase in the number of X-ray sources with a radio counterpart in a deep radio survey as the X-ray AGNs became progressively more obscured (but see Tozzi et al. 2009). Breaking down the μJy radio counts into contributions from different X-ray obscuring columns requires a detailed model of the circumnuclear star-forming region and will be the subject of future work.

In summary, the increased radio continuum sensitivity of the EVLA and the SKA will prove extremely powerful in the study of AGN evolution. Models of the 1.4 GHz number counts derived from a fit to the hard X-ray background show that the μJy population of AGNs will be dominated by radio-quiet, obscured Seyfert galaxies at $z \sim 1$. In addition, the radio fluxes from these AGNs may be enhanced by galactic star-formation. Indeed, current estimates of the AGN contribution to the 1.4 GHz radio counts seems to require moderate levels of star-formation in order for the models to match the observed data points. Multiwavelength followup observations of AGNs selected by their μJy radio emission will be able to trace the evolution of Seyfert galaxies from $z \sim 3$ to the present day.

The author thanks V. Smolčić, P. Padovani, N. Seymour and F. Bauer for useful conversations and comments. The anonymous referee is acknowledged for a detailed and constructive report.

REFERENCES

- Akylas, A., Georgantopoulos, I., Georgakakis, A., Kitsionas, S. & Hatziminaoglou, E., 2006, *A&A*, 459, 693
- Ballantyne, D.R., 2008, *ApJ*, 685, 787
- Ballantyne, D.R. & Papovich, C., 2007, *ApJ*, 660, 988
- Ballantyne, D.R., Everett, J.E. & Murray, N., 2006, *ApJ*, 639, 740
- Barger, A.J., Cowie, L.L., Mushotzky, R.F., Yang, Y., Wang, W.-H., Steffen, A.T. & Capak, P., 2005, *AJ*, 129, 578
- Bell, E.F., 2003, *ApJ*, 586, 794
- Benn, C.R., Rowan-Robinson, M., McMahon, R.G., Broadhurst, T.J. & Lawrence, A., 1993, *MNRAS*, 263, 98
- Beswick, R.J., Muxlow, T.W.B., Thrall, H., Richards, A.M.S. & Garrington, S.T., 2008, *MNRAS*, 385, 1143
- Blundell, K.M., Beasley, A.J., Lacy, M., & Garrington, S.T., 1996, *ApJ*, 468, L91
- Bondi, M. et al., 2003, *A&A*, 403, 857

- Bondi, M., Cilegi, P., Schinnerer, E., Smolčić, V., Jahnke, K., Carilli, C. & Zamorani, G., 2008, *ApJ*, 681, 1129
- Brandt, W.N. & Hasinger, G., 2005, *ARA&A*, 43, 827
- Bridle, A.H. & Perley, R.A., 1984, *ARA&A*, 22, 319
- Brinkmann, W., Laurent-Muehleisen, S.A., Voges, W., Siebert, R.H., Becker, R.H., Brotherton, M.S., White, R.L. & Gregg, M.D., 2000, *A&A*, 356, 445
- Condon, J.J., 1984, *ApJ*, 287, 461
- Condon, J.J., 1989, *ApJ*, 338, 13
- Condon, J.J., 1992, *ARA&A*, 30, 575
- Davies, R.I., Mueller Sánchez, F., Genzel, R., Tacconi, L.J., Hicks, E.K.S., Friedrich, S. & Sternberg, A., 2007, *ApJ*, 671, 1388
- Donley, J.L., Rieke, G.H., Pérez-González, P.G. & Barro, G., 2008, 687, 111
- Donoso, E., Best, P.N. & Kauffmann, G., 2009, *MNRAS*, 392, 617
- Dwelly, T. & Page, M.J. 2006, *MNRAS*, 372, 1755
- Fabian, A.C., Barcons, X., Almaini, O. & Iwasawa, K., 1998, *MNRAS*, 297, L11
- Fomalont, E.B., Kellermann, K.I., Cowie, L.L., Capak, P., Barger, A.J., Partridge, R.B., Windhorst, R.A. & Richards, E.A., 2006, *ApJS*, 167, 103
- Gabor, J.M., et al., 2009, *ApJ*, 691, 705
- Garn, T. & Alexander, P., 2009, *MNRAS*, 394, 105
- Georgakakis, A., Hopkins, A.M., Afonso, J., Sullivan, M., Mobasher, B. & Cram, L.E., 2004, *MNRAS*, 354, 127
- Gilli, R., Comastri, A. & Hasinger, G., 2007, *A&A*, 463, 79
- Grogin, et al., 2005, *ApJ*, 627, L97
- Gruppioni, C., Pozzi, F., Zamorani, G., Ciliegi, P., Lari, C., Calbrese, E., La Franca, F. & Matute, I., 2003, *MNRAS*, 341, L1
- Hasinger, G., 2008, *A&A*, 490, 905

- Hazard, C., Mackey, M.B. & Shimmins, A.J., 1963, *Nature*, 197, 1037
- Heckman, T.M., Ptak, A., Hornschemeier, A. & Kauffmann, G., 2005, *ApJ*, 634, 161
- Hickox, R.C. et al., 2009, *ApJ*, in press (arXiv:0901.4121)
- Ho, L., 2008, *ARA&A*, 46, 475
- Hopkins, A.M., 2004, *ApJ*, 615, 209
- Hopkins, A.M. & Beacom, J.F., 2006, *ApJ*, 651, 142
- Hopkins, A.M., Mobasher, B., Cram, L. & Rowan-Robinson, M., 1998, *MNRAS*, 296, 839
- Hopkins, A.M., Alfonso, J., Chan, B., Cram, L.E., Georgakakis, A., Mobasher, B., 2003, *AJ*, 125, 465
- Hopkins, P.F., Hernquist, L., Martini, P., Cox, T.J., Roberston, B., Di Matteo, T. & Springel, V., 2005, *ApJ*, 625, L71
- Huynh, M.T., Jackson, C.A., Norris, R.P. & Prandoni, I., 2005, *AJ*, 130, 1373
- Hutchings, J.B. & Neff, S.G., 1992, *AJ*, 104, 1
- Ibar, E. et al., 2008, *MNRAS*, 386, 953
- Jarvis, M.J. & Rawlings, S., 2004, *New A Rev.*, 48, 1173
- Kauffmann, G. & Haehnelt, M., 2000, *MNRAS*, 311, 576
- Kauffmann, G., et al., 2003, *MNRAS*, 346, 1055
- Kellermann, K.I. & Owen, F.N., 1988, in *Galactic and Extragalactic Radio Astronomy*, ed. G.L. Verschuur & K.I. Kellermann (2d ed.; New York: Springer), 563
- Kellermann, K.I., Fomalont, E.B., Maineri, V., Padovani, P., Rosati, P., Shaver, P., Tozzi, P. & Miller, N., 2008, *ApJS*, 179, 71
- Kim, M., Ho, L.C. & Im, M., 2006, *ApJ*, 642, 702
- Kukula, M.J., Dunlop, J.S., Hughes, D.H. & Rawlings, S., 1998, *MNRAS*, 297, 366
- La Franca, F. et al., 2005, *ApJ*, 635, 864
- Lawrence, A., 1991, *MNRAS*, 252, 586

- Longair, M.S., 1966, MNRAS, 133, 421
- Lynden-Bell, D, 1969, Nature, 223, 690
- Matthews, T.A. & Sandage, A.R., 1963, ApJ, 138, 30
- Moran, E.C., Filippenko, A.V. & Chornock, R., 2002, ApJ, 579, L71
- Mushotzky, R.F., in *Astrophysics and Space Science Library*, Vol. 308, *Supermassive Black Holes in the Distant Universe*, ed. A.J. Barger (Dordrecht: Kluwer), 53
- Napier, P.J., 2006, in *Revealing the Molecular Universe: One Antenna is Never Enough*, ed. D.C. Backer, J.W. Moran, & J.L. Turner (San Francisco: Astronomical Society of the Pacific), ASP Conf. Ser., 356, 65
- O’dea, C.P., 2002, *New A Rev.*, 46, 41
- Padovani, P., Mainieri, V., Tozzi, P., Kellermann, K.I., Fomalont, E.B., Miller, N., Rosati, P. & Shaver, P., 2009, ApJ, 694, 235
- Panessa, F., Barcons, X., Bassani, L., Cappi, M., Carrera, F.J., Ho, L.C. & Pellegrini, S., 2007, A&A, 467, 519
- Pierce, C.M. et al., 2007, ApJ, 660, L19
- Richards, E.A., 2000, ApJ, 533, 611
- Richards, A.M.S. et al., 2007, A&A, 472, 805
- Salpeter, E.E., 1964, ApJ, 140, 796
- Schinnerer, E. et al., 2007, ApJS, 172, 46
- Schmidt, M., 1963, Nature, 197, 1040
- Schawinski, K., Virani, S., Simmons, B., Urry, C.M., Treister, E., Kaviraj, S. & Kushkuley, B.A., 2009, ApJ, 692, L19
- Serjeant, S. & Hatziminaoglou, E., 2009, MNRAS, in press (arXiv:0901.0552)
- Seymour, N., McHardy, I.M. & Gunn, K.F., 2004, MNRAS, 352, 131
- Seymour, N., Dwelly, T., Moss, D., McHardy, I., Zoghbi, A., Rieke, G., Page, M., Hopkins, A. & Loaring, N., 2008, MNRAS, 386, 1695

- Shi, Y., Ogle, P., Rieke, G.H., Antonucci, R., Hines, D.C., Smith, P.S., Low, F.J., Bouwman, J. & Willmer, C., 2007, *ApJ*, 669, 841
- Sikora, M., Stawarz, L., Lasota, J.-P., 2007, *ApJ*, 658, 815
- Silverman, J.D., et al., 2008a, *ApJ*, 675, 1025
- Silverman, J.D., et al., 2008b, *ApJ*, 679, 118
- Silverman, J.D. et al., 2009, *ApJ*, in press (arXiv:0810.3653)
- Simpson, C., 2005, *MNRAS*, 360, 565
- Simpson, C., Martínez-Sansigre, A., Rawlings, S., Ivison, R., Akiyama, M., Sekiguchi, K., Takata, T., Ueda, Y. & Watson, M., 2006, *MNRAS*, 372, 741
- Smolčić, V. et al., 2008, *ApJS*, 177, 14
- Solomon, P.M. & Sage, L.J., 1988, *ApJ*, 642, 702
- Spergel, D.N., et al., 2003, *ApJS*, 148, 175
- Terashima, Y. & Wilson, A.S., 2003, *ApJ*, 583, 145
- Thompson, T.A., Quataert, E. & Murray, N., 2005, *ApJ*, 630, 167
- Tozzi, P. et al., 2009, *ApJ*, in press (arXiv:0902.2930)
- Treister, E. & Urry, C.M., 2006, *ApJ*, 652, L79
- Treister, E., Krolik, J.H. & Dullemond, C., 2008, *ApJ*, 679, 140
- Tueller, J., Mushotzky, R.F., Barthelmy, S., Cannizzo, J.K., Gehrels, N., Markwardt, C.B., Skinner, G.K. & Winter, L.M., 2008, *ApJ*, 681, 113
- Ueda, Y., Akiyama, M., Ohta, K. & Miyaji, T., 2003, *ApJ*, 598, 886
- Wada, K. & Norman, C., 2002, *ApJ*, 566, L21
- Watabe, Y., Kawakatu, N. & Imanishi, M., 2008, *ApJ*, 677, 895
- White, R.L., Becker, R.H., Helfand, D.J., & Gregg, M.D., 1997, *ApJ*, 475, 479
- Wilman, R.J., et al., 2008, *MNRAS*, 388, 1335
- Windhorst, R.A., Miley, G.K., Owen, F.N., Kron, R.G. & Koo, D.C., 1985, *ApJ*, 289, 494

Windhorst, R.A., Fomalont, E.B., Kellermann, K.I., Partridge, R.B., Richards, E.A., Franklin, B.E., Pascarella, S.M. & Griffiths, R.E., 1995, *Nature*, 375, 471

Winter, L.M., Mushotzky, R.F., Reynolds, C.S. & Tueller, J., 2009, *ApJ*, 690, 1322

Yun, M.S., Reddy, N.A. & Condon, J.J., 2001, *ApJ*, 554, 803

Zakamska, N.L. et al., 2003, *AJ*, 126, 2125

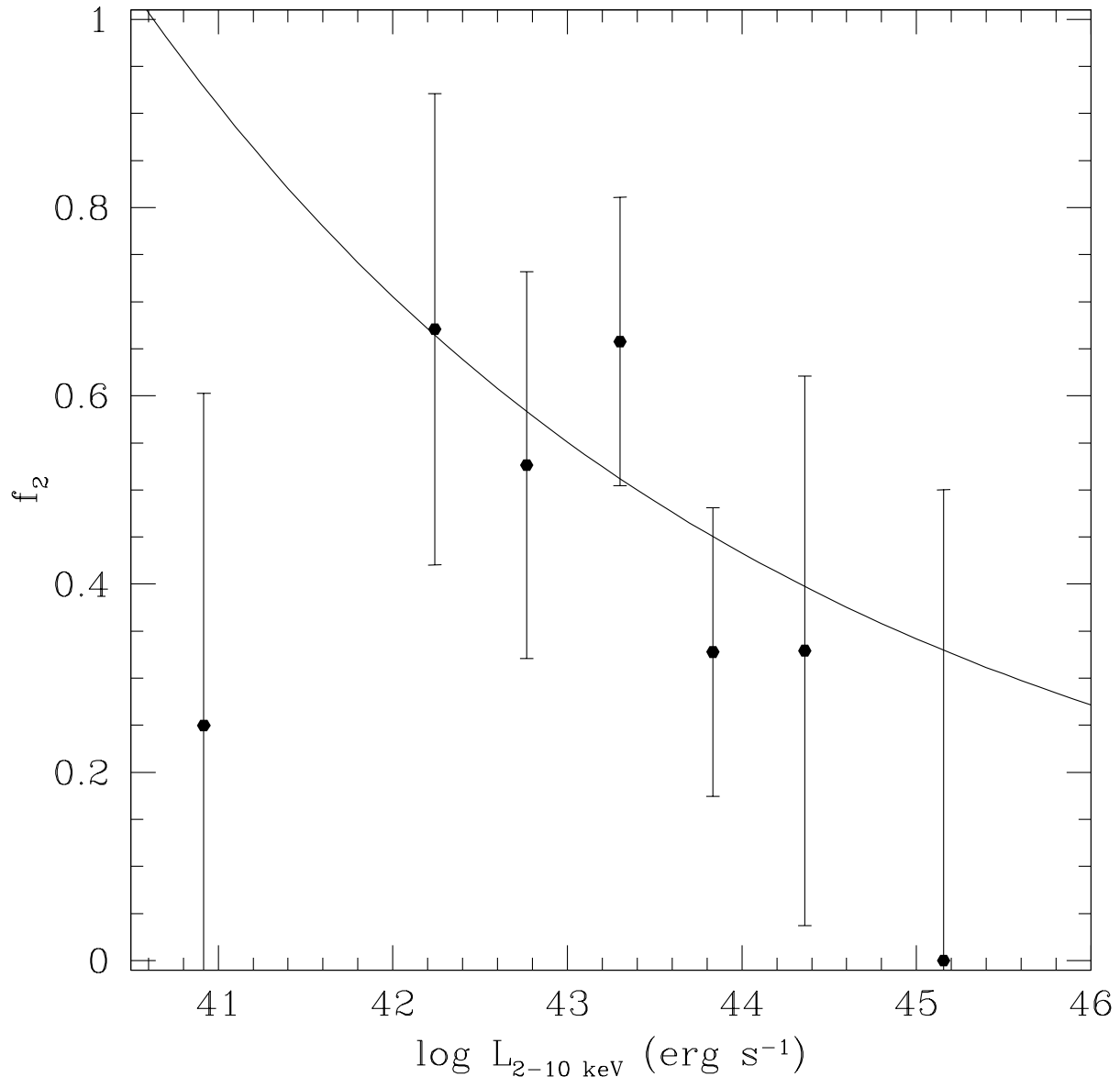


Fig. 1.— The fraction of type 2 AGNs as a function of L_X as determined by the *Swift*/BAT survey of Tueller et al. (2008). The observed correlation between L_X and $L_{14-195 \text{ keV}}$ (Winter et al. 2009) was used to convert the luminosities to the L_X band. The solid line is a power-law fit to the data assuming a 4:1 type 2/type 1 ratio at $\log L_X = 41.5$. The best fit has a reduced $\chi^2 = 0.97$ and follows $f_2 \propto \log L_X^{-10.5}$.

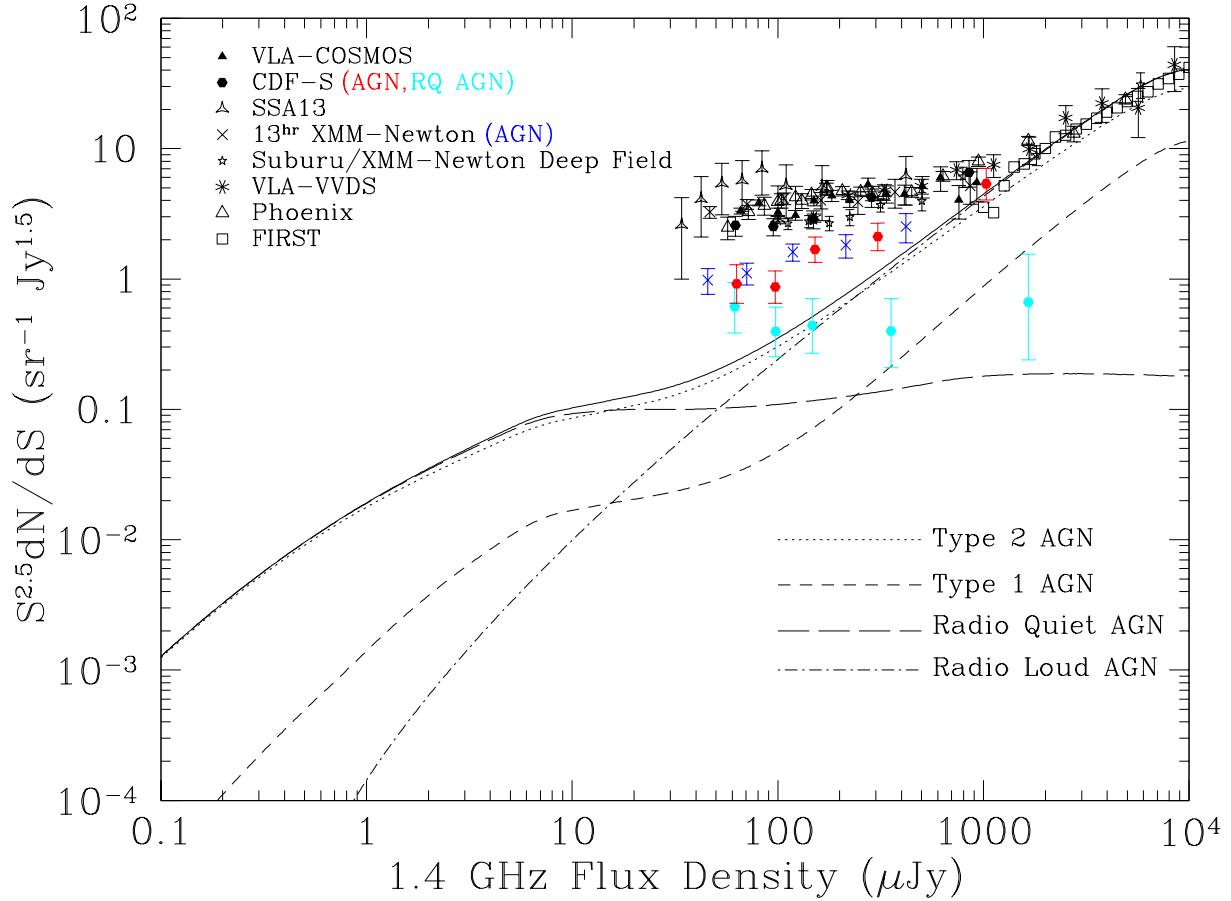


Fig. 2.— The solid line plots the predicted Euclidean-normalized 1.4 GHz radio counts from 0.1 μJy to 10 mJy obtained from the X-ray background modeling described in Section 2. The dotted and short-dashed lines plot the contribution to the counts from obscured and unobscured AGNs, respectively. These curves include AGNs of all radio powers. Type 2 AGNs dominate both the radio-loud and radio-quiet populations at these flux levels. The contribution from radio-quiet AGNs is plotted as the long-dashed line, while radio-loud AGNs are shown as the dot-dashed line. These curves include both obscured and unobscured AGNs. The points indicate the observed counts obtained from various surveys: VLA-COSMOS (Bondi et al. 2008), CDF-S (Kellermann et al. 2008), SSA13 (Fomalont et al. 2006), 13hr *XMM-Newton* (Seymour et al. 2004), Suburu/*XMM-Newton* Deep Field (Simpson et al. 2006), VLA-VVDS (Bondi et al. 2003), Phoenix (Hopkins et al. 2003) and FIRST (White et al. 1997). The blue and red data plot the estimated AGN contribution to the radio counts from the 13hr *XMM-Newton* (Seymour et al. 2008) and CDF-S (Padovani et al. 2009) surveys, respectively. The cyan data points are estimates of the radio-quiet AGN contribution in the CDF-S (Padovani et al. 2009).

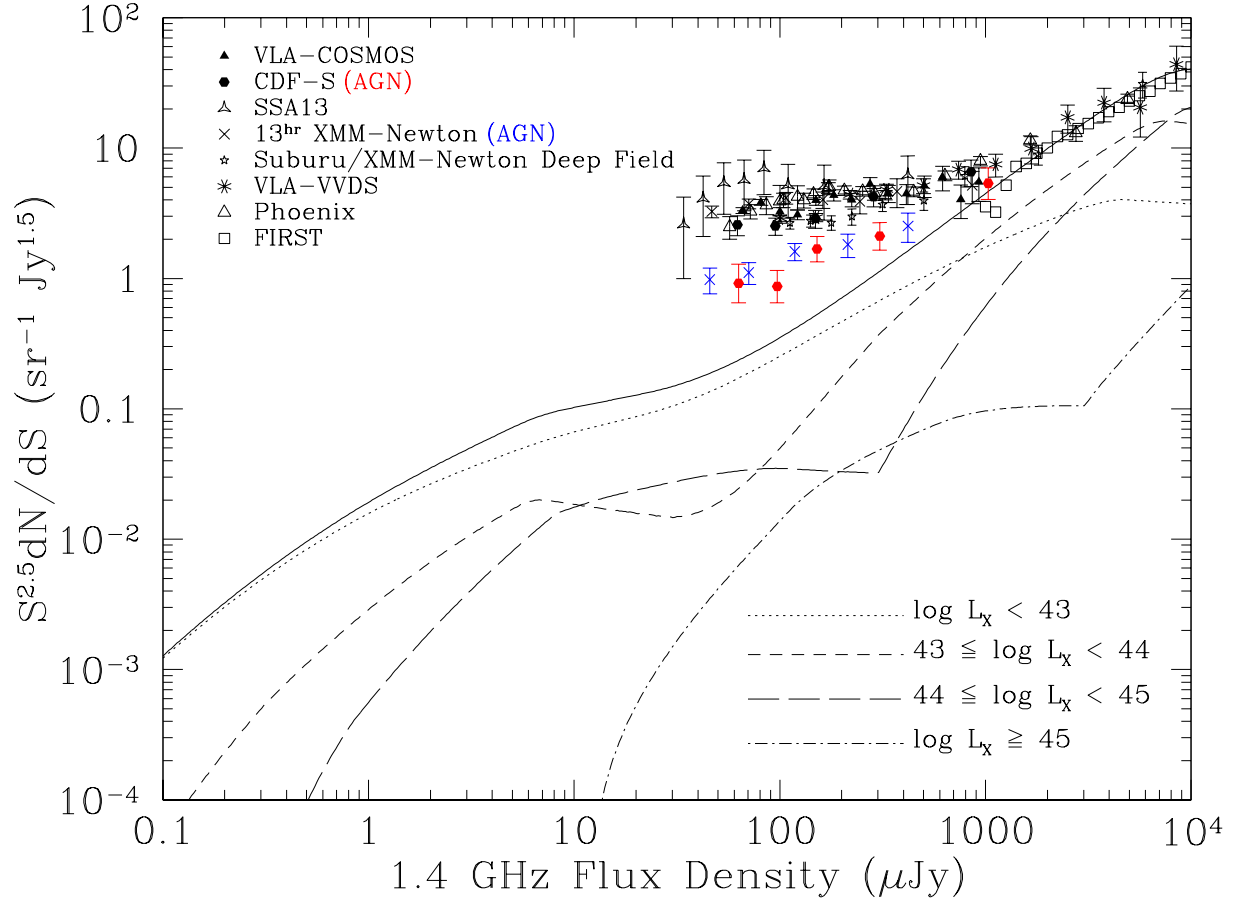


Fig. 3.— As in Figure 2, but the contributions to the total number counts from AGNs with different absorption-corrected X-ray luminosities are now indicated.

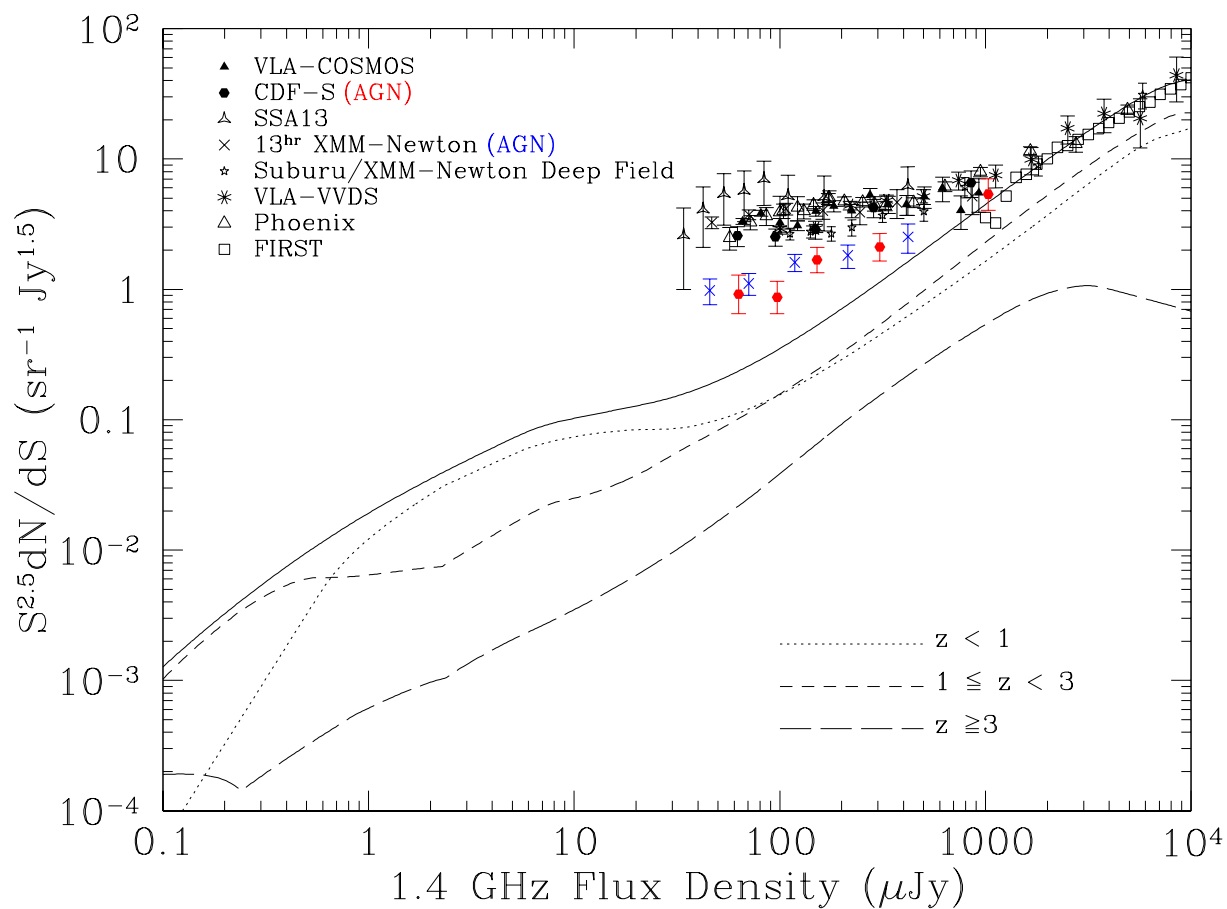


Fig. 4.— As in Figure 2, but the contributions to the total number counts from AGNs at different redshifts are now indicated.

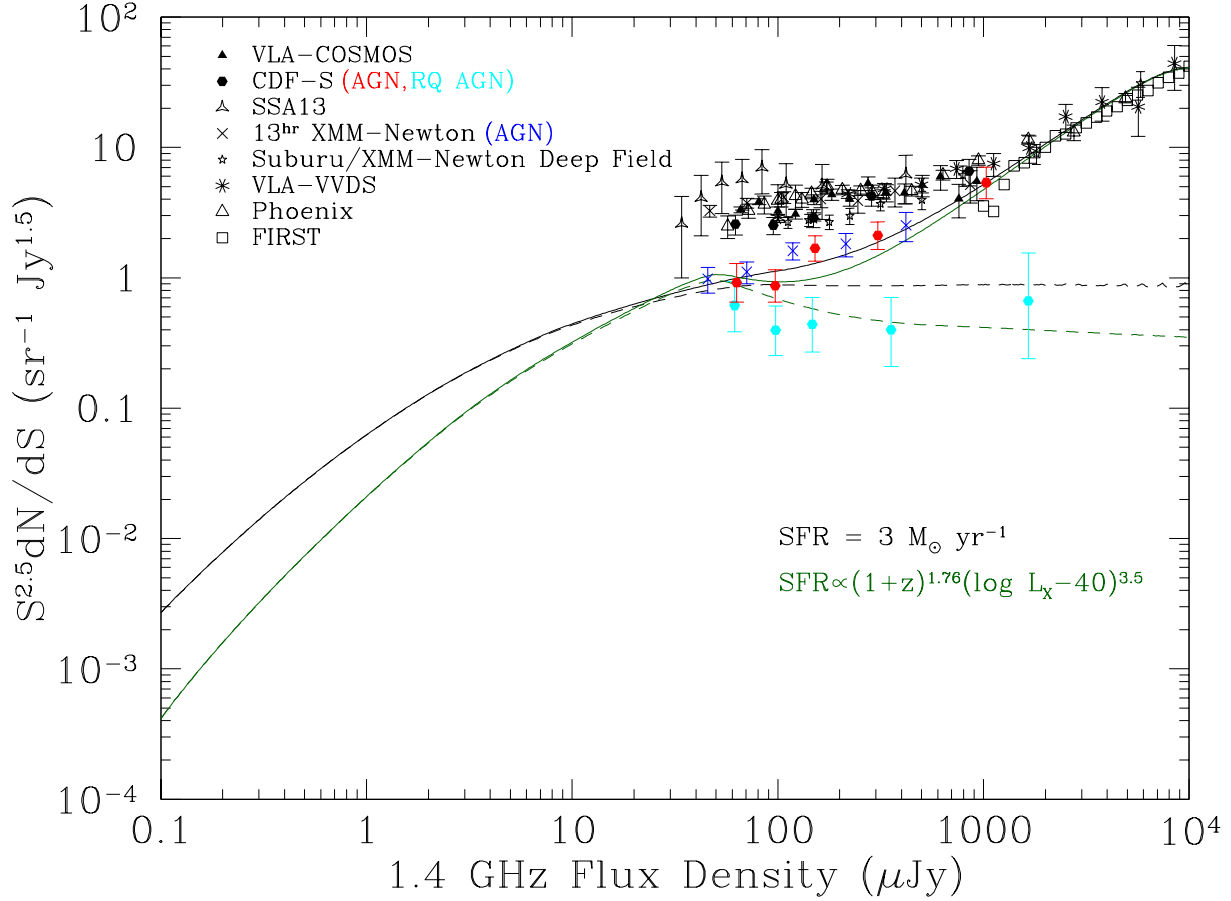


Fig. 5.— The black solid line plots the predicted number counts from AGNs including radio emission from a constant SFR of $3 M_{\odot} \text{ yr}^{-1}$. The black dashed line shows the contribution from radio-quiet AGNs in this scenario. The green lines are the analogous curves for a model where the SFR is a function of both $\log L_X$ and z (eq. 5). In both cases the radio emission was added to only the type 2 AGNs. The data points are the same as in Fig. 2.

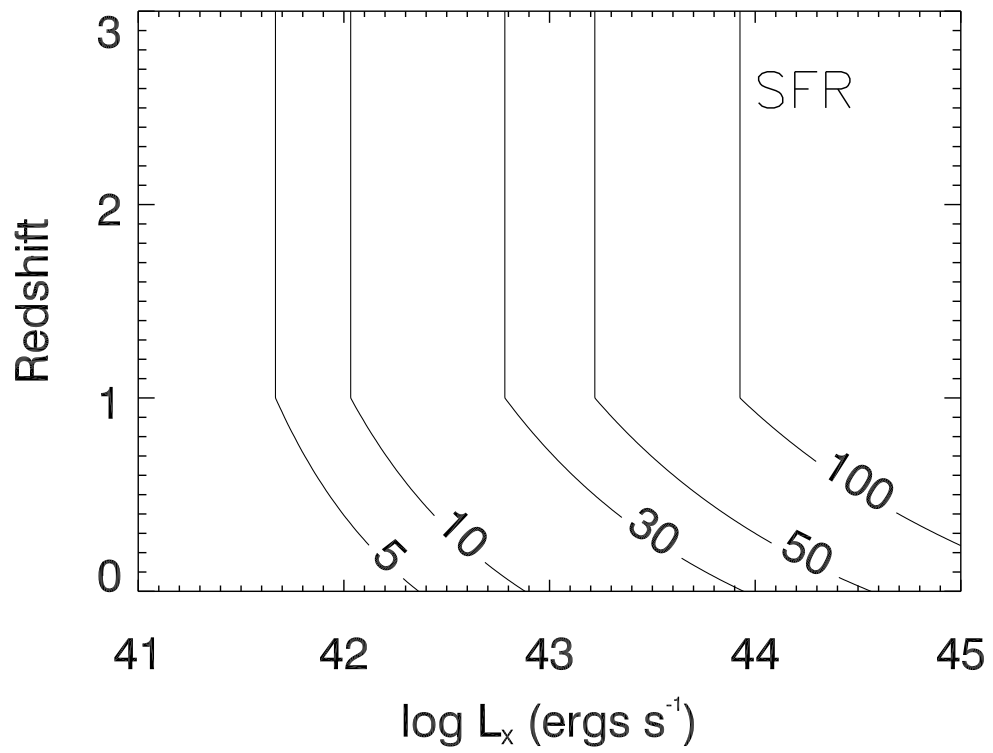


Fig. 6.— Contours of SFR in $M_{\odot} \text{ yr}^{-1}$ as a function of $\log L_X$ and z calculated using equation 5. This law indicates that SFRs $\lesssim 30 M_{\odot} \text{ yr}^{-1}$ may be common in the host galaxies of the μJy AGN population.

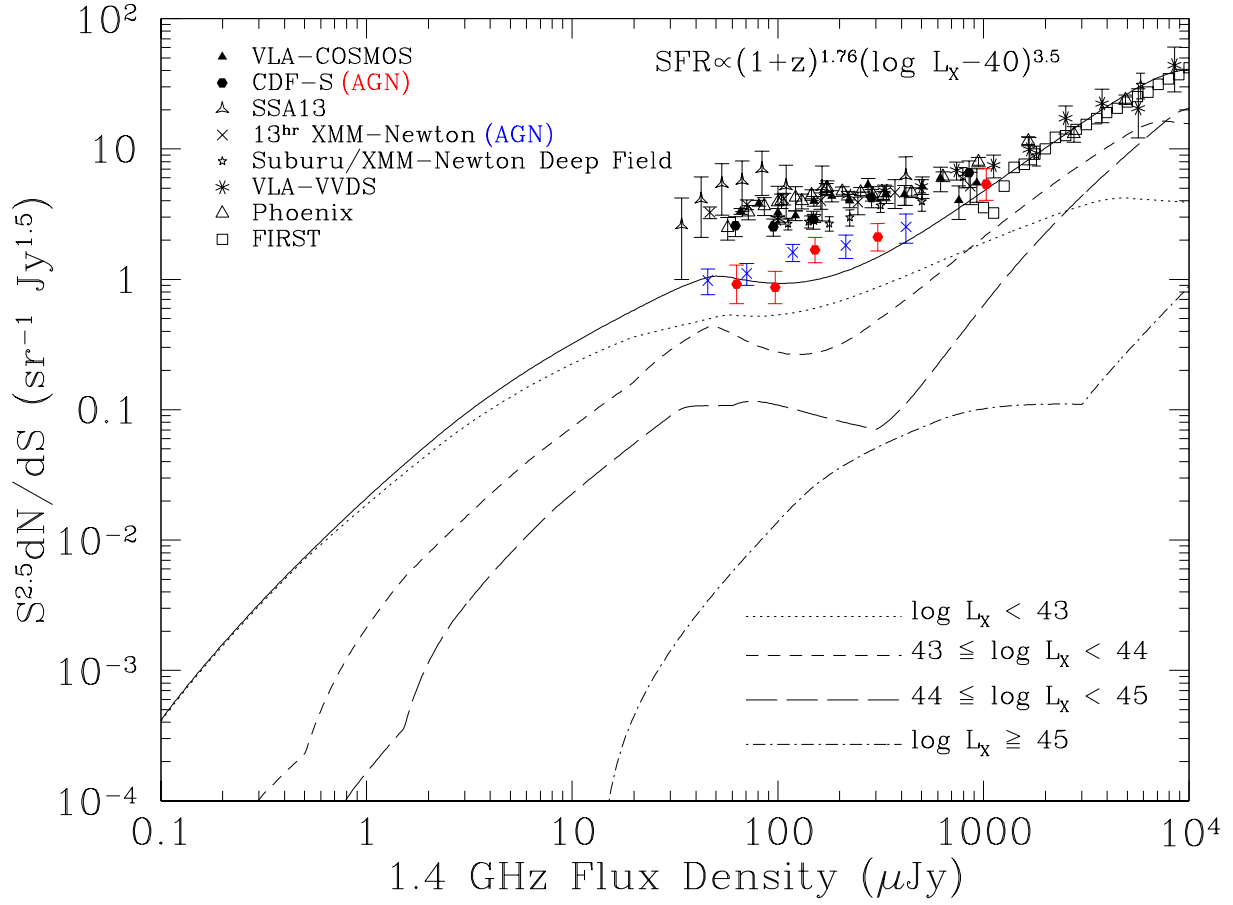


Fig. 7.— As in Figure 3, but radio flux from a SFR given by eq. 5 was added to the type 2 AGNs.

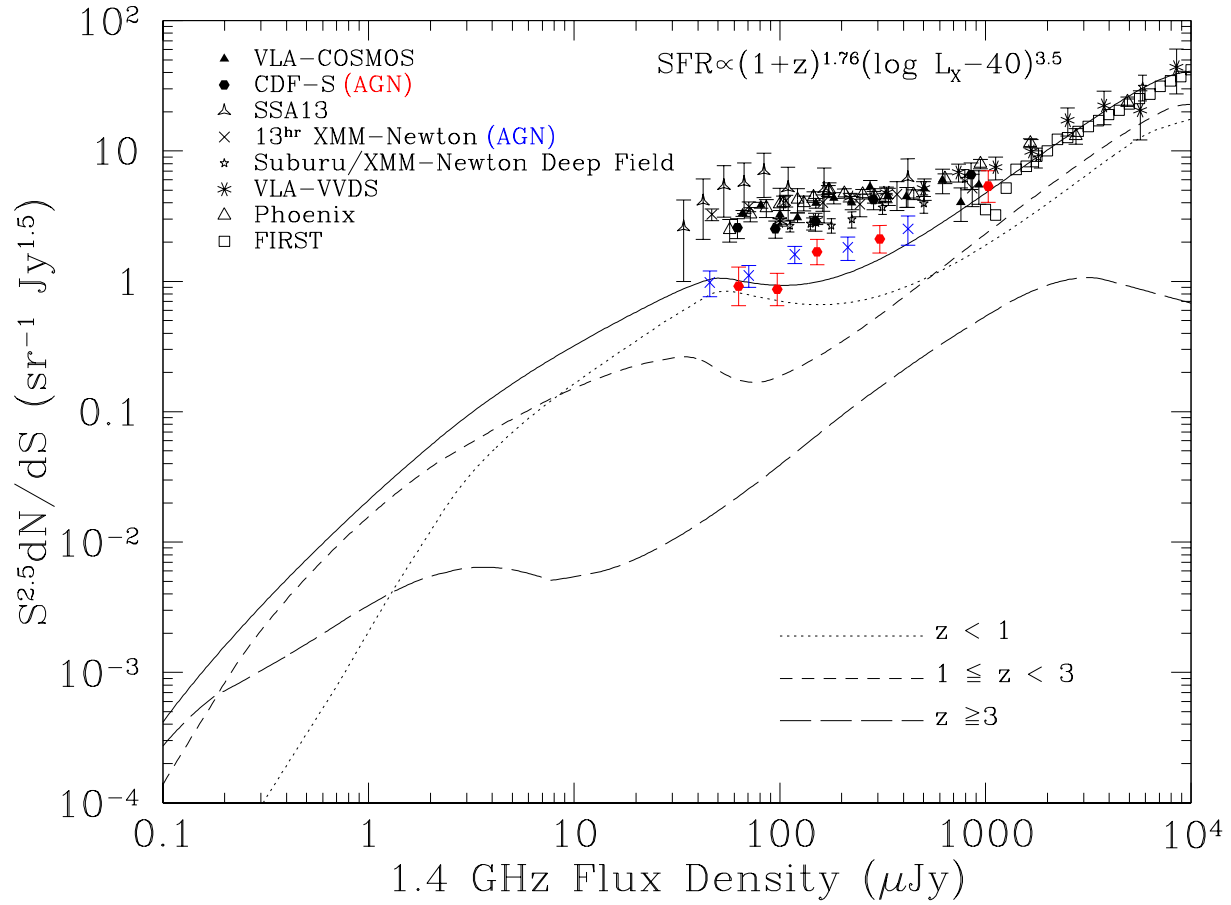


Fig. 8.— As in Figure 4, but radio flux from a SFR given by eq. 5 was added to the type 2 AGNs.

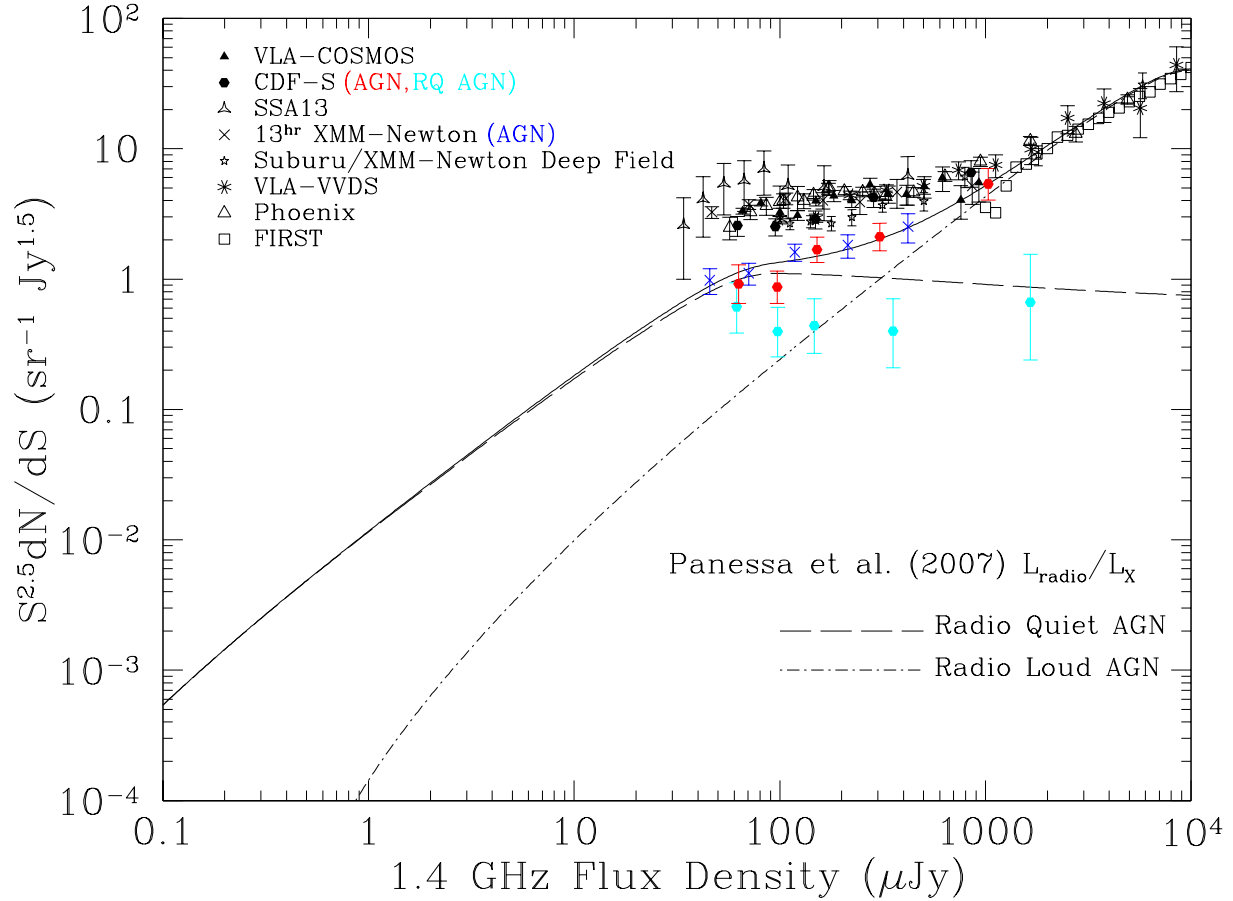


Fig. 9.— The solid line plots the predicted number counts due to AGNs when assuming the Panessa et al. (2007) relationship between L_X and $\nu L_\nu(5 \text{ GHz})$. No additional emission from star-forming regions has been included. The contributions from radio-quiet and radio-loud AGNs are shown as indicated.

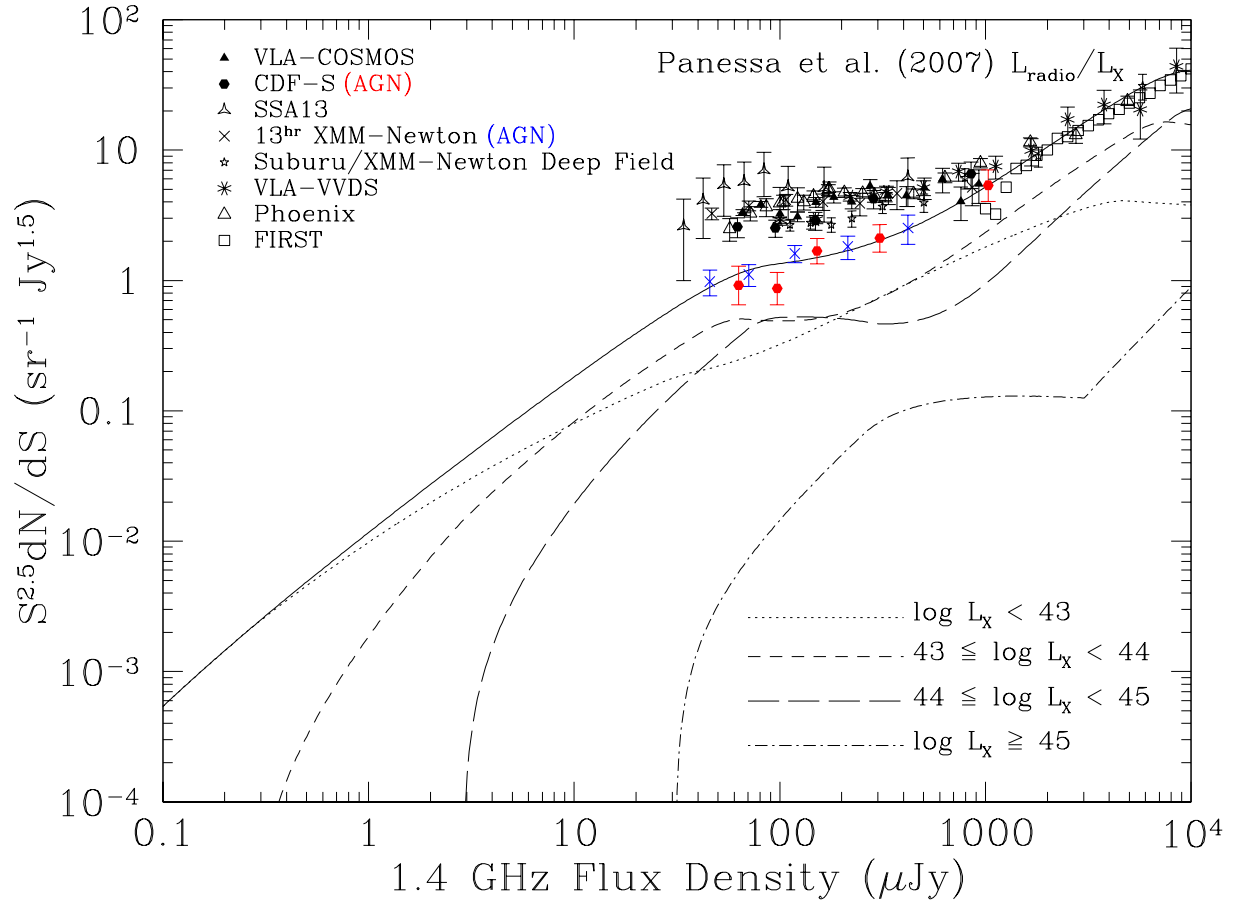


Fig. 10.— As in Figure 9, but the contributions to the total number counts from AGNs with different absorption-corrected X-ray luminosities are now indicated.

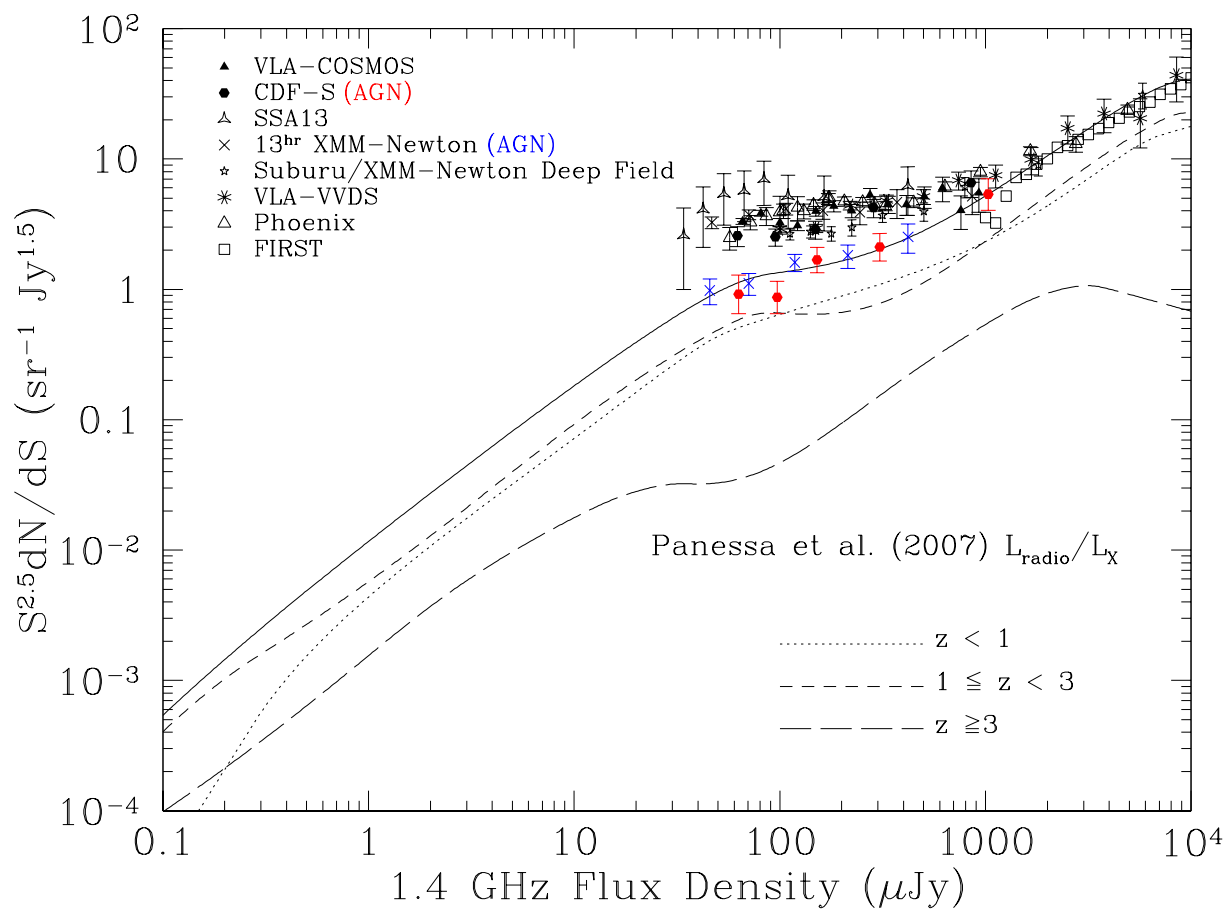


Fig. 11.— As in Figure 9, but the contributions to the total number counts from AGNs at different redshifts are now indicated.